Journal of Organometallic Chemistry 694 (2009) 3190–3199

Contents lists available at ScienceDirect

Journal of Organometallic Chemistry

journal homepage: www.elsevier.com/locate/jorganchem

fac-Acetato-bis(pyrazole) complexes: A systematic study on intra- and intermolecular hydrogen bonds

Marta Arroyo, M. Teresa García-de-Prada, Carolina García-Martín, Vanesa García-Pacios, Raúl García-Rodríguez, Patricia Gómez-Iglesias, Fernando Lorenzo, Isaac Martín-Moreno [1], Daniel Miguel, Fernando Villafañe *

IU CINQUIMA/Química Inorgánica, Facultad de Ciencias, Universidad de Valladolid, 47005 Valladolid, Spain

ARTICLE INFO

Article history:
Received 6 May 2009
Accepted 7 May 2009
Available online 15 May 2009

Keywords:
Hydrogen bonds
Pyrazole
Carboxylate ligands
Molybdenum
Group 7 metals

ABSTRACT

Acetato-bis(pyrazole) complexes [Mo(η^3-methallyl)(O_2CMe)$(CO)_2$($pz^*H)_2$], (methallyl = $CH_2C(CH_3)CH_2$) and *fac*-[$M(O_2CMe)(CO)_3(pz^*H)_2$], (pz^*H = pyrazole or 3,5-dimethylpyrazole, dmpzH; M = Mn, Re) are obtained from [Mo(η^3-methallyl)$Cl(CO)_2(NCMe)_2$] or *fac*-[$MBr(CO)_3(NCMe)_2$] [M = Mn (synthesized *in situ*), Re], 2 equiv. of pyrazole, and 1 equiv. of sodium acetate for Mo complexes, or silver acetate for Mn or Re complexes. The chlorido-complexes [Mo(η^3-methallyl)$Cl(CO)_2L_2$] (L = pzH, dmpzH), obtained from the same starting material by substitution of MeCN by pzH or dmpzH, are also described. The crystal structures of the *fac*-acetato-bis(dimethylpyrazole) complexes present the same pattern of intramolecular hydrogen bonds between the acetate and the dimetylpyrazole ligands, whereas the crystal structures of the *fac*-acetato-bis(pyrazole) complexes show different hydrogen bonds patterns, with intermolecular interactions. NMR data indicate that these interactions are not maintained in solution.

1. Introduction

One of the main features of pyrazole complexes is the involvement of the N-bound hydrogen of pyrazole in intra- or intermolecular hydrogen bonds. Their crystal structures rarely show intermolecular hydrogen-bonded chains or oligomers [1,2], and frequently exhibit intramolecular hydrogen-bonds, or hydrogen-bonding to solvent molecules or counterions. In fact, cationic pyrazole complexes have been recently used as anion receptors in solution [3].

The presence in the same complex of pyrazoles and other ligands able to behave as hydrogen bond acceptor allows a systematic study of which factors determine the formation of inter- and/or intramolecular interactions. This is one of the big challenges of chemistry, that is, the understanding and control of the organization of molecules [4]. Hydrogen bonded organic aggregates have so far been object of main attention, but the presence of metals in supramolecular systems is attracting increasing interest, as they may show redox [5], optical [6], magnetic [7], adsorption [8], or catalytical [9] properties. We considered that complexes containing the *fac*-"$MX(pz^*H)_2$" (X = halogen, pz^*H = any pyrazole) moiety [10] could be good precursors to start this study, if the halogen is replaced by another ligand able to establish hydrogen bonding interactions with the hydrogens of pyrazoles. The *fac* geometry of these complexes, caused by the relative donor-accepting properties of the ligands, allows this study, as no other geometric factors are involved. The acetate was chosen to play this role, since the oxygens may act as hydrogen acceptors, and this interaction may determine the coordination behavior of the acetate, as has been recently demonstrated [11].

2. Results and discussion

2.1. Synthesis of the complexes

The complexes herein described were obtained by the reactions depicted in Scheme 1.

Chlorido-bis(pyrazole) complexes [Mo(η^3-methallyl)$Cl(CO)_2$-$(pzH)_2$] (**1a**) and [Mo(η^3-methallyl)$Cl(CO)_2(dmpzH)_2$] (**1b**) were obtained by treating [Mo(η^3-methallyl)$Cl(CO)_2(NCMe)_2$] with 2 equiv. of pzH or dmpzH in CH_2Cl_2 at room temperature (Scheme 1) [12].

The molybdenum complexes [Mo(η^3-methallyl)(O_2CMe)$(CO)_2$-$(pzH)_2$] (**2a**) and [Mo(η^3-methallyl)(O_2CMe)$(CO)_2(dmpzH)_2$] (**2b**) were obtained from [Mo(η^3-methallyl)$Cl(CO)_2(NCMe)_2$], 2 equiv. of the pyrazole and sodium acetate (Scheme 1). The reactions occur readily at room temperature in THF. Obviously, **1a** or **1b** may be considered as intermediates in the self-assembly method, as has been demonstrated in a separated experiment for **1a**, which was also ob-

* Corresponding author. Tel.: +34 983 184620; fax: +34 983 323013.
E-mail address: fervilla@qi.uva.es (F. Villafañe).
[1] Deceased.

0022-328X/$ - see front matter © 2009 Elsevier B.V. All rights reserved.
doi:10.1016/j.jorganchem.2009.05.006

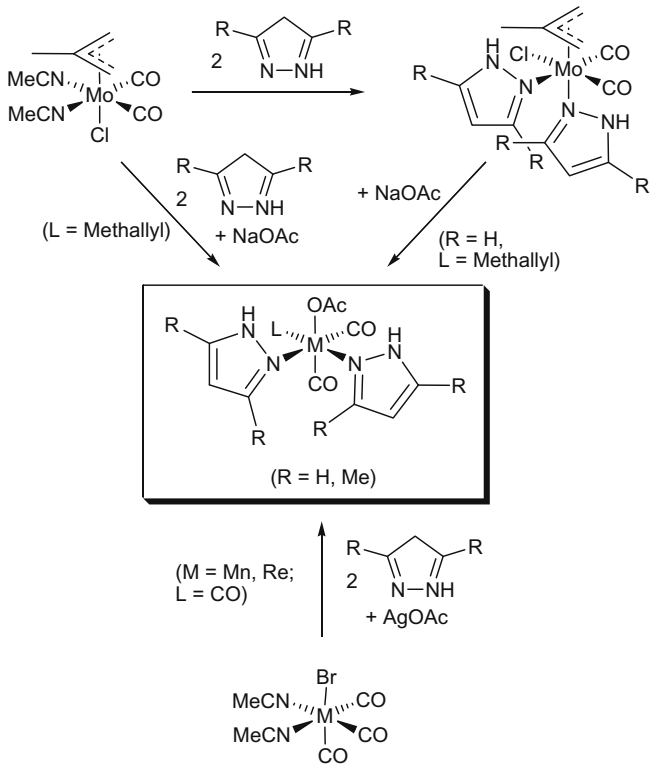

Scheme 1. Syntheses of chlorido and acetato complexes.

tained from the addition of 2 equiv. of pyrazole to [Mo(η^3-methallyl)Cl(CO)$_2$(NCMe)$_2$] (Scheme 1).

The manganese and rhenium complexes *fac*-[M(O_2CCH_3)-(CO)$_3$(pzH)$_2$] (M = Mn, **3a**; M = Re, **4a**) and *fac*-[M(O_2CCH_3)-(CO)$_3$(dmpzH)$_2$] (M = Mn, **3b**; M = Re, **4b**) were obtained by a similar method but using AgOAc instead of NaOAc as halogen extractor.

2.2. Solid-state structural characterization

The structures of **1a** and **1b** [13] are shown in Fig. 1, and Table 1 collects relevant distances and angles.

The molybdenum atoms are pseudo-octahedrally coordinated, assuming that the methallyl group occupies one site. The terminal carbon atoms of the methallyl groups point towards the carbonyl groups, as has been demonstrated to be the most energetically favorable arrangement [14]. The distances and angles are very similar to those found in the previously reported structures of pyrazolemolybdenum(II) complexes with different halogen or allyl groups [10b,15]. One of the pyrazole ligands is coordinated *trans* to the methallyl group in all these structures, as opposite to what is usually found in complexes of the type [MoX(η^3-allyl)(CO)$_2$L$_2$] (X = halide or pseudo halide, L$_2$ = nitrogen donor ligand), where the nitrogen donor ligands are *trans* to the carbonyls [16].

The N-bound hydrogens are involved in intramolecular hydrogen bonds with the chlorine atom [H(2)···Cl(1) 2.351 Å and H(4)···Cl(1) 2.257 Å for **1a** and 2.034 and 2.018 for **1b**]. These, and the corresponding N···Cl distances [3.119 Å and 3.041 Å for **1a**, and 2.681 and 2.649, respectively, for **1b**], and N–H···Cl angles [130° and 132° for **1a**, 118° and 117° for **1b**] confirm the presence of a hydrogen bond which may be considered between "weak" and "moderate" for **1a**, or "moderate" for **1b** [17,18]. The structures of **2a** and **2b** are shown, respectively, in Figs. 2 and 3, whereas relevant distances and angles are collected in Table 2 [19]. Both structures present the usual pseudooctahedral geometry of

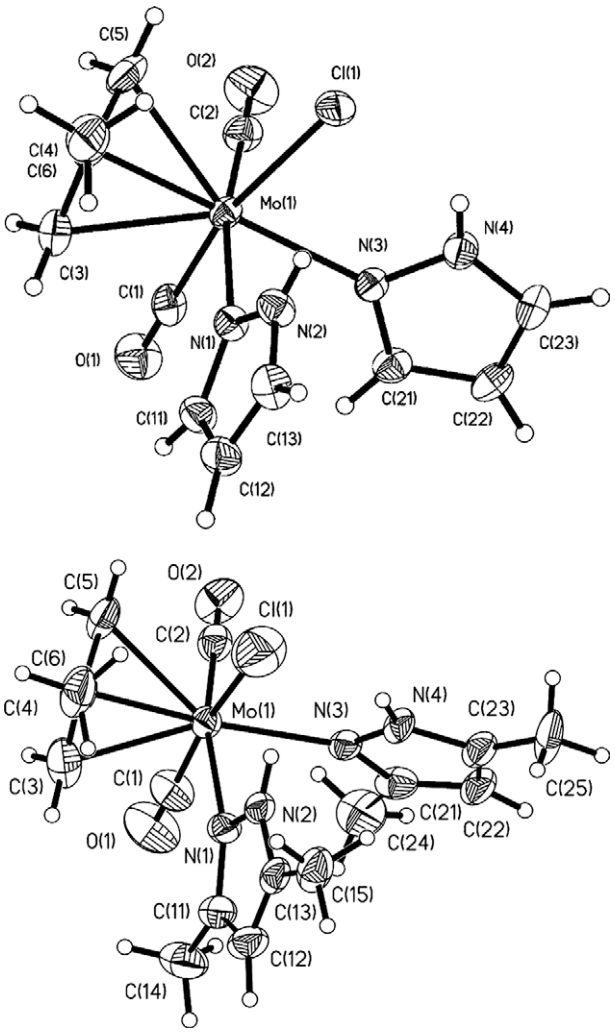

Fig. 1. Perspective views of [Mo(η^3-methallyl)Cl(CO)$_2$(pzH)$_2$], **1a** (above), and [Mo(η^3-methallyl)Cl(CO)$_2$(dmpzH)$_2$], **1b** (below), showing the atom numbering.

Table 1
Selected distances (Å) and angles (deg.) for [Mo(η^3-methallyl)Cl(CO)$_2$(pzH)$_2$], **1a**, and [Mo(η^3-methallyl)Cl(CO)$_2$(dmpzH)$_2$], **1b**.

	1a	1b
Mo(1)–C(1)	1.943(3)	1.93(2)
Mo(1)–C(2)	1.943(3)	1.943(19)
Mo(1)–N(1)	2.254(2)	2.281(13)
Mo(1)–N(3)	2.246(2)	2.232(12)
Mo(1)–Cl(1)	2.5788(8)	2.156(8)
Mo(1)–C(4)	2.237(3)	2.220(16)
Mo(1)–C(3)	2.345(3)	2.326(18)
Mo(1)–C(5)	2.311(3)	2.303(16)
C(2)–Mo(1)–C(1)	81.99(12)	77.4(7)
C(2)–Mo(1)–N(1)	168.36(11)	166.6(6)
C(1)–Mo(1)–N(1)	94.54(10)	99.0(7)
C(2)–Mo(1)–N(3)	88.66(11)	86.8(6)
C(1)–Mo(1)–N(3)	86.68(10)	95.2(7)
N(1)–Mo(1)–N(3)	80.03(8)	80.6(4)
C(2)–Mo(1)–Cl(1)	97.03(9)	102.9(5)
C(1)–Mo(1)–Cl(1)	167.98(9)	173.3(6)
N(1)–Mo(1)–Cl(1)	84.05(6)	79.1(4)
N(3)–Mo(1)–Cl(1)	81.31(6)	78.2(4)

(η^3-methallyl)molybdenum complexes, with the open face of the allyl moiety oriented over the carbonyls. As evidenced by Table 2, the distances and angles are very similar in both complexes, and

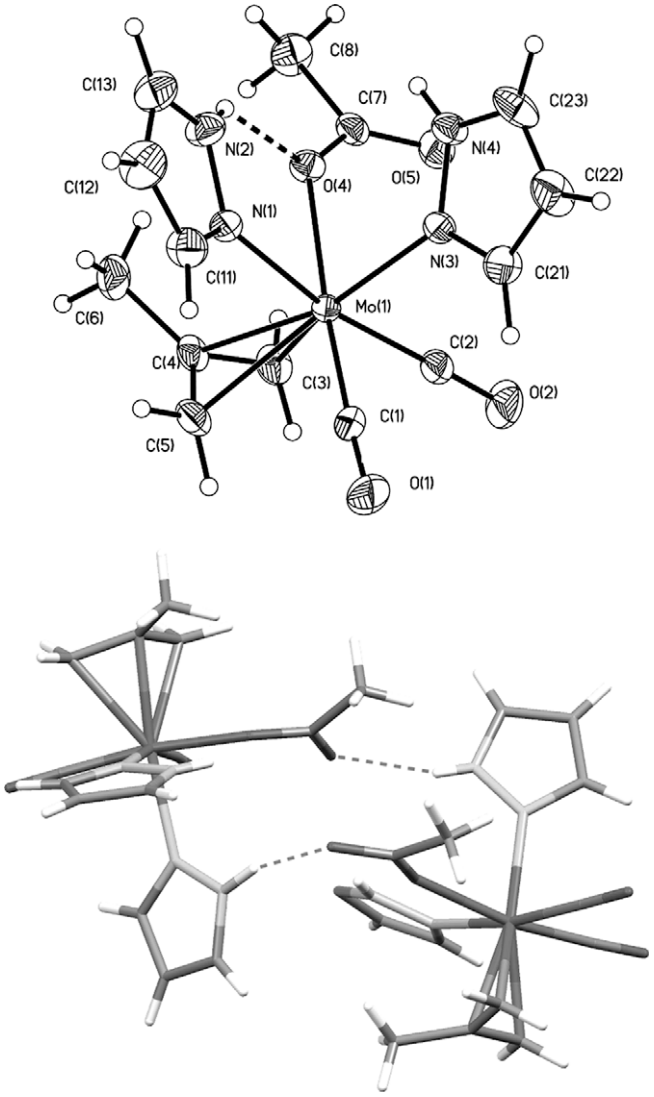

Fig. 2. Perspective view showing the atom numbering (above), and intermolecular hydrogen bonds (below) of [Mo(η^3-methallyl)(O_2CMe)(CO)$_2$(pzH)$_2$], **2a** (below), showing the atom numbering.

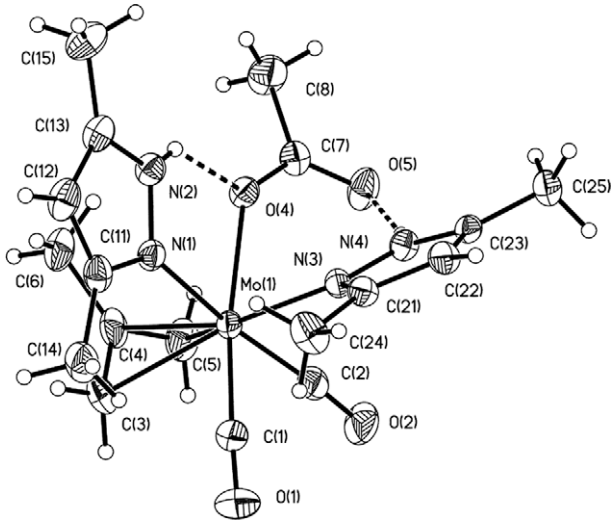

Fig. 3. Perspective view of [Mo(η^3-methallyl)(O_2CMe)(CO)$_2$(dmpzH)$_2$], **2b**, showing the atom numbering.

Table 2
Selected distances (Å) and angles (deg.) for [Mo(η^3-methallyl)(O_2CMe)(CO)$_2$(pzH)$_2$], **2a**, and [Mo(η^3-methallyl)(O_2CMe)(CO)$_2$(dmpzH)$_2$], **2b**.

	2a	2b
Mo(1)–C(1)	1.924(4)	1.937(4)
Mo(1)–C(2)	1.946(4)	1.953(4)
Mo(1)–N(1)	2.271(3)	2.283(3)
Mo(1)–N(3)	2.229(3)	2.259(3)
Mo(1)–O(4)	2.175(3)	2.223(3)
Mo(1)–C(4)	2.239(4)	2.232(3)
Mo(1)–C(3)	2.313(4)	2.331(3)
Mo(1)–C(5)	2.327(4)	2.317(4)
C(2)–Mo(1)–C(1)	79.51(18)	78.24(16)
C(2)–Mo(1)–N(1)	166.29(15)	169.14(12)
C(1)–Mo(1)–N(1)	98.20(15)	98.85(13)
C(2)–Mo(1)–N(3)	86.52(15)	87.02(13)
C(1)–Mo(1)–N(3)	89.10(15)	89.96(13)
N(1)–Mo(1)–N(3)	79.90(11)	82.49(11)
C(2)–Mo(1)–O(4)	103.24(15)	101.29(12)
C(1)–Mo(1)–O(4)	171.79(15)	170.03(12)
N(1)–Mo(1)–O(4)	77.27(11)	79.74(9)
N(3)–Mo(1)–O(4)	83.39(11)	80.06(9)

similar to those described above for **1a** and **1b** or for the previously reported structures of bis(pyrazole)halodicarbonylmolybdenum(II) complexes [10b,15]. As occur in these structures, one of the pyrazole ligands is coordinated *trans* to the allyl group.

Two intramolecular hydrogen bonds are detected in **2b** (Fig. 3): between the coordinated oxygen of the acetate and the N-bound hydrogen of one of the dmpzH ligands [H(2)···O(4) 1.961 Å], and between the uncoordinated oxygen of the acetate and the N-bound hydrogen of the second dmpzH [H(4)···O(5) 1.787 Å]. These and the corresponding N···O distances (2.696 and 2.789 Å, respectively) and N–H···O angles (126° and 163°, respectively) confirm the presence of a hydrogen bond which may be considered as "moderate" [17]. This pattern (Fig. 4) is observed in all the complexes containing dmpzH and acetate described herein. However, only one intramolecular hydrogen bond is detected for **2a** (Fig. 2 above): that between the coordinated oxygen of the acetate and the N-bound hydrogen of one of the pzH ligands [H(2)···O(4) 1.908, with distances N(2)···O(4) 2.670, and N–H···O angle 128°]. The N-bound hydrogen of the second pzH is involved in a moderate intermolecular hydrogen bond with the uncoordinated oxygen of the acetate of a second molecule, giving rise to the dimer depicted in Fig. 2 (below) [H(4)···O(55) 1.750, H(54)···O(5) 1.806 Å, with distances N(4)···O(55) 2.745, N(54)···O(5) 2.793 Å, and N–H···O angles 161° and 159°, respectively]. Both intra- and intermolecular values correspond again to "moderate" hydrogen bonds [17].

The relative orientation of the pyrazole ligands differs in each complex: dmpzH ligands are tilted in the same direction in **2b** (46(1)° for the dmpzH involved in the intramolecular bond with the uncoordinated oxygen of the acetate, and 12(1)° for the other

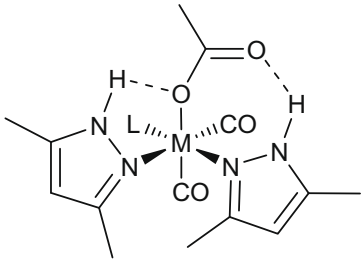

Fig. 4. Hydrogen bond pattern observed in the crystal structures of the complexes containing dmpzH and acetate [L = (η^3-methallyl), M = Mo (**2b**); L = CO, M = Mn (**3b**), Re (**4b**)].

dmpzH), whereas pzH ligands in **2a** are symmetrically tilted respect to the plane perpendicular to that containing the metal and the nitrogen donor atoms (−14(1)° and 7(1)°, respectively). Therefore, the intra- or intermolecular nature of the hydrogen bond seems to determine the orientation of the pyrazole ligand involved in it. Steric factors might also influentiate this feature, as the structures of complexes containing two dmpzH coordinated *cis* usually show higher distortions than those with pzH [10]. In fact, the deviations shown by the pzH ligands in the chlorido-complexes are clearly lower: 10(1)° and −1(1)° for **1a**, and 10(1)° and −5(1)° for **1b**. The structures of the manganese and rhenium complexes **3a**, **3b**, **4a**, and **4b** were also determined by X-ray diffraction, and the results are shown in Figs. 5 (**3a**), 6 (**4a**), and 7 (**3b** and **4b**). Distances and angles in these structures (those relevant are collected in Table 3) are similar to those found in previously reported structures of pyrazolemanganese(I) and -rhenium(I) complexes, which are scarce, and show a slightly distorted octahedral geometry [10a,10c,20]. These distortions are evidenced by the slight deviation from the ideal angles shown by the ligands coordinated *trans* or *cis* (see Table 3).

The intramolecular hydrogen bonds detected the complexes with dmpzH **3b** and **4b** (Fig. 7) follow the same pattern than those described above for **2b** (depicted in Fig. 4): the coordinated oxygen of the acetate is hydrogen-bonded to the N-bound hydrogen of one of the dmpzH ligands [H(2)···O(4) 2.381 Å for **3b** and 2.334 Å for **4b**, with N···O distances 2.794 Å and 2.803 Å, and N–H···O angles 103° and 106°, respectively], and the uncoordinated oxygen of the acetate is hydrogen-bonded the N-bound hydrogen of the second dmpzH [H(4)···O(5) 1.925 Å for **3b** and 1.796 Å for **4b**, with N···O distances 2.716 Å and 2.717, and N–H···O angles 164° and 147°, respectively]. These distances confirm the presence of a hydrogen bond which may be considered between "weak" and "moderate" [17].

Whereas one intra- and other intermolecular hydrogen bond were detected for **2a** (Fig. 2), only intermolecular bonds are found in **3a**: both N-bound hydrogens of each molecule are hydrogen-bonded to the uncoordinated oxygen of an adjacent molecule, forming a chain structure (Fig. 5). The distances indicate that these hydrogen bonds may be considered as "moderate" [17]: 2.095 Å for H(2)···O(5) and 1.953 Å for H(4)···O(5), being 3.055 Å for N(2)···O(5) and 2.910 Å for N(4)···O(5), with N–H···O angles 154° and 153°, respectively.

A different pattern from those found in the structures of **2a** and **3a** is detected in **4a**: in this case, the uncoordinated oxygen of the acetate is involved in two hydrogen bonds, one intramolecular with one of the pyrazoles [H(4)···O(5) 1.880 Å, N(4)···O(5) 2.765 Å, and N–H···O 142°], and another intermolecular with the pyrazole of other molecule not involved in intramolecular hydrogen bonding [H(2)···O(5) 1.702 Å, and N(2)···O(5) 2.720 Å, and N–H···O 169°] (Fig. 6). These distances point to hydrogen bonds which may be considered as "moderate" [17].

The pyrazole ligands in the structures of **3a**, **3b**, **4a**, and **4b** are tilted around the Mo–N bonds. In these structures each pair of pyrazole ligands is orientated in the same direction respect to the plane perpendicular to that containing the metal and the nitrogen donor atoms, being the averaged angles 25(1)° and 23(1)° for **3a**, 43(1)° and 38(1)° for **3b**, 50(1)° and 44(1)° for **4a**, and 31(1)° and 50(1)° for **4b**. It should be noted that these angles are rather similar in the three structures, as opposite to what is observed in those of **2a** and **2b** (see above).

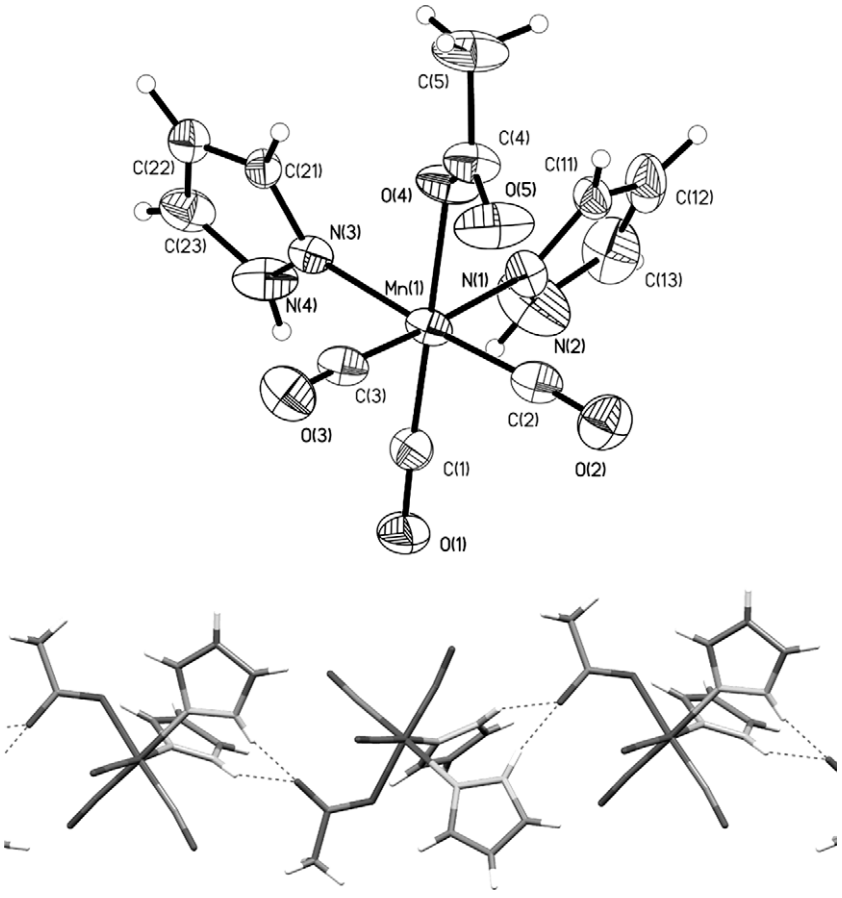

Fig. 5. Perspective view showing the atom numbering (above), and hydrogen bonds (below) of *fac*-[Mn(O_2CMe)(CO)$_3$($pzH)_2$], **3a**.

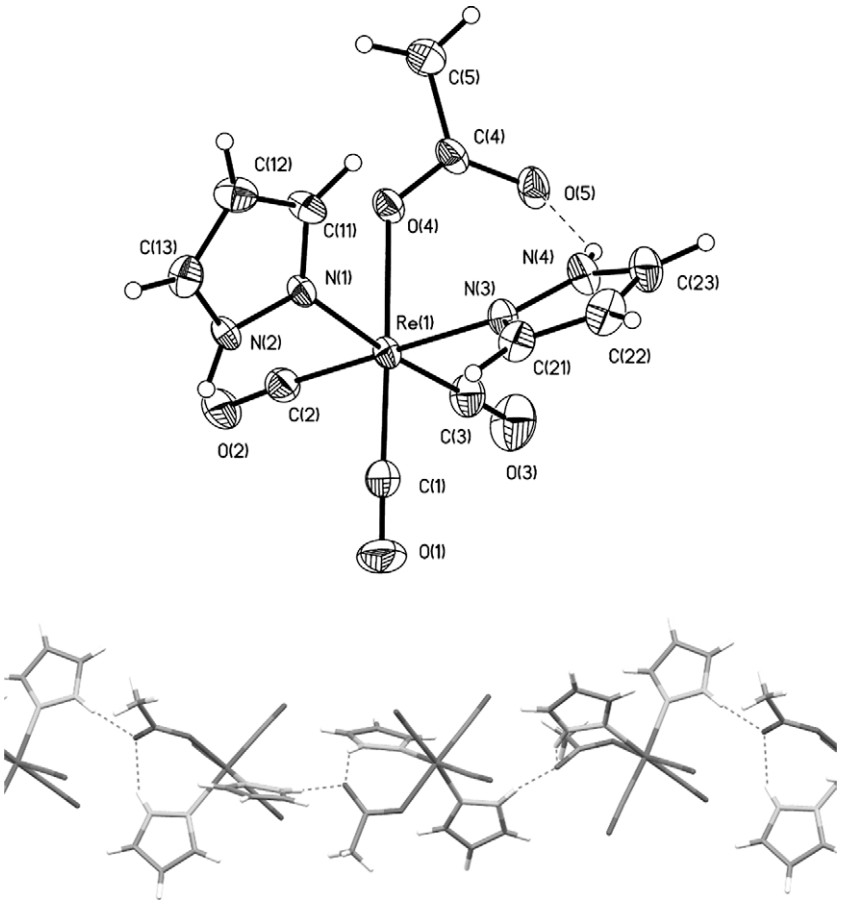

Fig. 6. Perspective view showing the atom numbering (above), and hydrogen bonds (below) of *fac*-[Re(O_2CMe)$(CO)_3(pzH)_2$], **4a**.

2.3. Characterization in solution

The IR spectra of all the complexes show two bands in the C–O stretching region in solution for the molybdenum complexes and three for the manganese and rhenium complexes, as expected for their respective *cis*-dicarbonyl and *fac*-tricarbonyl geometries. The frequencies are higher for complexes with pzH than those with dmpzH, and for manganese than for rhenium complexes. Both features are to be expected considering the higher electronic density of the third row vs. first row transition metal series, and the better donor properties of dmpzH compared to pzH [21].

As indicated above, complexes of the type [Mo(η^3-$CH_2C(R)HCH_2$)$X(CO)_2L_2$] [R = H (allyl), Me (methallyl); X = halide or pseudo halide; L_2 = two monodentate ligands or a bidentate ligand] may be considered as pseudo-octahedral if the η^3-allyl ligand is considered as occupying one coordination position. Considering only the most favorable arrangement, where the terminal atoms of the allyl group are oriented over the carbonyl groups [14], there are two possible geometries for these complexes: **S** or symmetric, where the pyrazoles are coordinated in the *equatorial* positions, *trans* to the carbonyls; and **A** or asymmetric, where one of the pyrazoles is coordinated *trans* to the allyl group, in the *axial* position (Fig. 8).

Molybdenum complexes **1a**, **1b**, **2a**, and **2b** show a dymanic behavior in solution similar to that observed for similar bromido-complexes with allyl instead of methallyl, which has been previously detailed [10b]. Although they crystallize as the asymmetric isomer **A** (Figs. 1 and 8), their ^{1}H and ^{13}C NMR spectra at room temperature show the equivalence of both methylenes of the methallyl group, and both pyrazoles, what points to the symmetric isomer **S**. The broadness of some signals suggests a slow exchange process in solution below the coalescence. Complexes [Mo(η^3-$CH_2C(R)HCH_2$)$X(CO)_2L_2$] usually display a non-dissociative trigonal twist process in which there is an intramolecular rotation of the XL_2 triangular face [22], which would lead to the equilibrium between the symmetric **S** and both enantiomers of the asymmetric **A**. Therefore, if this exchange process is fast enough, a symmetric average spectrum should be observed. As previously described [10b], other dynamic processes in solution detected for this type of complexes, such as the η^3–η^1–η^3 rearrangement of the allyl [23], or the "pivoted double switch" process [24], may be discarded.

The trigonal twist process observed for **1a** and **1b** is faster than those observed for the similar complexes [Mo(η^3-allyl)$Br(CO)_2L_2$] (L = pzH, dmpzH), which ^{1}H NMR spectra at the same field show averaged symmetric only at higher temperatures [10b]. The lower activation energy of methallyl respect to allyl complexes in the system [Mo(η^3-$CH_2C(R)HCH_2$)$X(CO)_2L_2$] has been already reported [25].

The broadness observed at room temperature for the NH protons might be due to a rapid prototropic exchange involving the pyrrolic proton, which is common in pyrazole complexes [26]. The assignment of the hydrogens or methyl groups in positions 3 and 5 is difficult when they display singlets, since their chemical shift seems to be affected by different factors, which are difficult to evaluate: whether the hydrogen (or methyl) group at position 3 resonates at higher field than 5 or *viceversa* may vary in the same family of complexes [27], or even depending on the solvent used [28]. When the complexes are fluxional the broader signals (those coalescing at higher temperatures) have been assigned to the

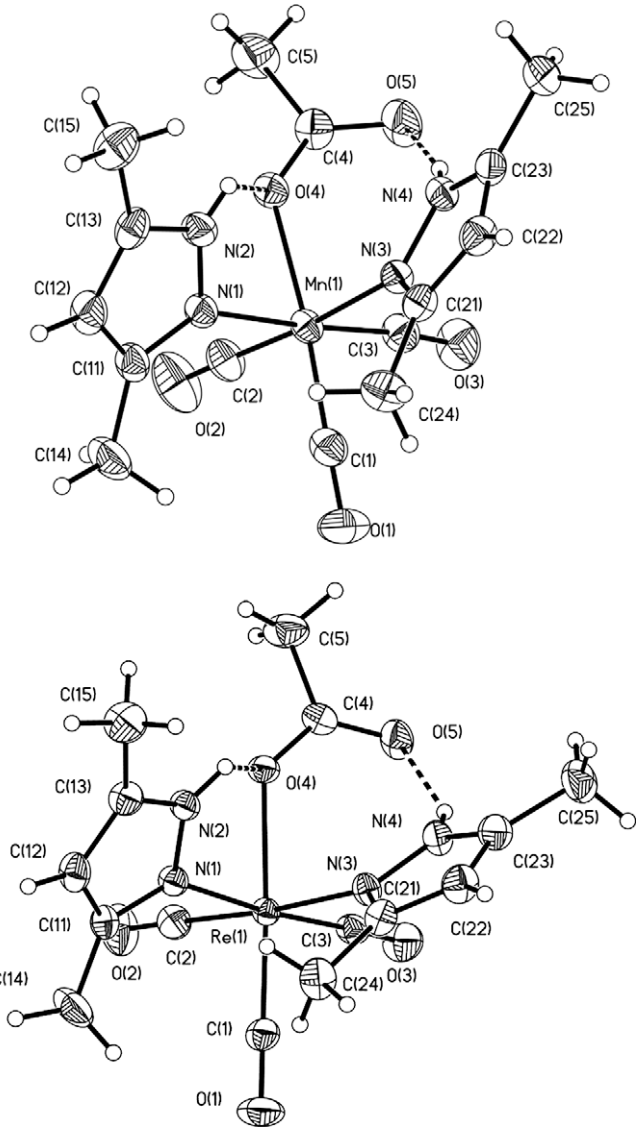

Fig. 7. Perspective views of *fac*-[Mn(O_2CMe)(CO)$_3$(dmpzH)$_2$], **3b** (above), and *fac*-[Re(O_2CMe)(CO)$_3$(dmpzH)$_2$], **4b** (below), showing the atom numbering.

group (H or Me) at position 3, as they are closer to the unequivalence source than those at position 5, which point to the outside of the complex. However, the assignment proposed for the rest of complexes in Section 4 may be considered as tentative.

The ^{1}H NMR spectrum of **3a** displays broad signals for the methyl of the acetate and for some pyrazole signals. When the spectrum is carried out at 223 K, no substantial sharpening is detected, probably because of the nuclear quadrupole moment of manganese. The ^{1}H NMR spectrum of **3a** at room temperature with an excess of sodium acetate shows only one singlet for the methyl groups of coordinated and free acetate, suggesting a process involving dissociation of the acetate ligand. The electrical conductivities of the acetato complexes in acetone solution are typical of non-electrolyte complexes, what point to very low dissociation degree.

The NH protons of the acetate complexes resonate at lower field (ca. 1 ppm) than those of similar halocomplexes [Mo(η^3-methallyl)Cl(CO)$_2$L$_2$] (**2**), *fac*-[MnBr(CO)$_3$L$_2$] [10a], or *fac*-[ReBr(CO)$_3$L$_2$] [10c]; (L = pzH. dmpzH), and this chemical shift is independent from the concentration. The last feature may be interpreted considering either (a) all the hydrogen bond interactions detected in the solid state structures are not maintained in solution, or (b) all the hydrogen bond interactions are intramolecular. As the solid state structures of the acetato-bis(pyrazole) complexes show intermolecular interactions, option (b) should be discarded.

Table 3
Selected distances (Å) and angles (°) for *fac*-[Mn(O_2CMe)(CO)$_3$(pzH)$_2$], **3a**, *fac*-[Mn(O_2CMe)(CO)$_3$(dmpzH)$_2$], **3b**, *fac*-[Re(O_2CMe)(CO)$_3$(pzH)$_2$], **4a**, and *fac*-[Re(O_2CMe)(CO)$_3$(dmpzH)$_2$], **4b**.

	3a (M = Mn)	**3b** (M = Mn)	**4a** (M = Re)	**4b** (M = Re)
M(1)–C(1)	1.781(5)	1.786(3)	1.894(5)	1.878(9)
M(1)–C(2)	1.796(6)	1.792(3)	1.908(5)	1.918(9)
M(1)–C(3)	1.793(5)	1.802(3)	1.926(5)	1.917(8)
M(1)–N(1)	2.069(4)	2.070(2)	2.178(3)	2.182(6)
M(1)–N(3)	2.069(4)	2.0792(19)	2.189(4)	2.195(6)
M(1)–O(4)	2.024(3)	2.0530(16)	2.156(3)	2.164(5)
C(1)–M(1)–C(2)	87.4(2)	89.30(12)	87.4(2)	87.6(4)
C(1)–M(1)–C(3)	89.3(2)	87.02(12)	88.1(2)	86.7(3)
C(2)–M(1)–C(3)	91.1(2)	89.10(11)	87.0(2)	89.5(4)
C(1)–M(1)–O(4)	177.05(17)	175.35(10)	174.95(17	177.3(3)
C(2)–M(1)–O(4)	94.68(19)	86.66(10)	94.95(16)	91.5(3)
C(3)–M(1)–O(4)	92.75(17)	95.22(9)	96.47(18)	95.9(3)
N(1)–M(1)–O(4)	84.42(15)	82.13(7)	78.88(12)	80.0(2)
N(3)–M(1)–O(4)	82.40(14)	89.07(7)	86.02(13)	84.5(2)
C(1)–M(1)–N(1)	93.50(18)	95.77(10)	96.44(17)	97.5(3)
C(2)–M(1)–N(1)	90.18(19)	92.82(10)	95.46(16)	93.4(3)
C(3)–M(1)–N(1)	176.97(19)	176.63(10)	174.91(18)	175.0(3)
O(4)–M(1)–N(1)	84.42(15)	82.13(7)	78.88(12)	80.0(2)
C(2)–M(1)–N(3)	176.15(18)	175.65(10)	177.81(16)	175.6(3)
C(1)–M(1)–N(3)	95.43(18)	94.93(10)	91.52(19)	96.3(3)
C(3)–M(1)–N(3)	91.52(19)	92.08(10)	94.89(18)	92.9(3)
O(4)–M(1)–N(3)	82.40(14)	89.07(7)	86.02(13)	84.5(2)
N(1)–M(1)–N(3)	87.05(13)	85.81(7)	82.79(13)	84.0(2)

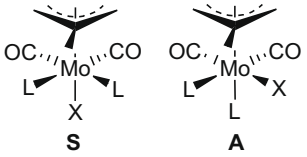

Fig. 8. Two possible geometries for complexes [Mo(η^3-CH_2C(R)HCH_2)X(CO)$_2$L$_2$].

3. Conclusions

The crystal structures of the complexes herein described containing one acetato and two dimetylpyrazole ligands in a *fac* geometry show the same pattern: intramolecular hydrogen bonds are detected between the N-bound hydrogen of one of the dmpzH ligands with the coordinated oxygen of the acetate, and between the N-bound hydrogen of the second dmpzH with the uncoordinated oxygen of the acetate. When similar complexes with pzH are obtained, their crystal structures do not show the same pattern, since intermolecular hydrogen bonds are detected. These arrangements of the three monodentate ligands observed in the solid state do not persist in solution, as indicate NMR data.

4. Experimental

4.1. General Remarks

All manipulations were performed under N_2 atmosphere following conventional Schlenk techniques. Filtrations were carried out on dry Celite under N_2. Solvents were purified according to standard procedures [29]. [Mo(η^3-methallyl)Cl(CO)$_2$(NCMe)$_2$] [30], *fac*-[MnBr(CO)$_3$(NCMe)$_2$] [10a], and *fac*-[ReBr(CO)$_3$(NCMe)$_2$] [31] were obtained as previously described. All other reagents

were obtained from the usual commercial suppliers, and used as received. Infrared spectra were recorded in a Perkin–Elmer RX I FT-IR apparatus using 0.2 mm CaF_2 cells for solutions or on KBr pellets for solid samples. NMR spectra were recorded in Bruker AC-300 or ARX-300 instruments in $CDCl_3$ at room temperature unless otherwise stated. NMR spectra are referred to the internal residual solvent peak for ^1H and $^{13}C\{^1H\}$ NMR. Assignment of the $^{13}C\{^1H\}$ NMR data was supported by DEPT experiments and relative intensities of the resonance signals. Electrical conductivity measurements were carried out at r.t. with a Crison 522 conductivimeter on ca. 5×10^{-4} M solutions; the range of molar conductivity for 1/1 electrolytes is 100–160 S cm^2 mol^{-1} in acetone solutions [32]. Elemental analyses were performed on a Perkin–Elmer 2400B microanalyzer.

4.2. [Mo(η^3-methallyl)Cl(CO)$_2$(pzH)$_2$] (**1a**)

[Mo(η^3-methallyl)Cl(CO)$_2$(NCMe)$_2$] (0.160 g, 0.5 mmol) was added to a solution of pzH (0.068 g, 1.0 mmol) in CH_2Cl_2 (20 mL). The solution was stirred at r.t. for 5 min and hexane was added (ca. 20 mL). Concentration of the solution in vacuo and cooling to −20 °C gave a yellow microcrystalline solid, which was decanted, washed with hexane (3 × 3 mL approximately), and dried in vacuo, yielding 0.172 g (91%). IR (THF, cm^{-1}): 1942 vs, 1845 s. IR (KBr, cm^{-1}): 3311 s, 3269 s, 3115 w, 1925 s, 1815 s, 1473 m, 1404 w, 1350 m, 1260 w, 1130 m, 1049 s, 1030 m, 788 m, 764 s, 734 w, 606 w. ^1H NMR (r.t.): 1.37 (s, H^{anti} methallyl, 2H), 1.92 (s, CH_3 methallyl, 3H), 3.25 (br, H^{syn} methallyl, 2H), 6.32 (br, H^4 pzH, 2H), 7.40 (s, H^5 pzH, 2H), 7.92 (br, H^3 pzH, 2H), 11.86 (br, N*H*, 2H). ^1H NMR (223 K): 1.27 (s, H^{anti} methallyl, 1H), 1.39 (s, H^{anti} methallyl, 1H), 1.86 (s, CH_3 methallyl, 3H), 3.00 (s, H^{syn} methallyl, 1H), 3.43 (s, H^{syn} methallyl, 1H), 6.25 (s, H^4 pzH, 1H), 6.40 (s, H^4 pzH, 1H), 7.40 (s, H^5 pzH, 2H), 7.56 (s, H^3 pzH, 1H), 8.26 (s, H^3 pzH, 1H), 11.78 (s, N*H*, 2H). $^{13}C\{^1H\}$ NMR: 20.0 (s, *C*H_3 methallyl), 58.8 (s, *C*H_2 methallyl), 83.0 (s, $CH_3C(CH_2)_2$), 107.0 (s, C^4 pzH), 128.8 (s, C^5 pzH), 143.0 (s, C^3 pzH), 225.4 (br, *C*O). Anal. Calcd. for $C_{14}H_{15}ClMoN_4O_2$: C, 38.06; H, 3.99; N, 14.79. Found: C, 38.32; H, 3.70; N, 14.83%.

4.3. [Mo(η^3-methallyl)Cl(CO)$_2$(dmpzH)$_2$] (**1b**)

[Mo(η^3-methallyl)Cl(CO)$_2$(NCMe)$_2$] (0.160 g, 0.5 mmol) was added to a solution of dmpzH (0.096 g, 1.0 mmol) in CH_2Cl_2 (20 mL). The solution was stirred at r.t. for 5 min, the volatiles were removed in vacuo, and the yellow residue was extracted with Et_2O (ca. 20 mL) and filtered. Hexane was added (ca. 20 mL) and the solution was concentrated and cooled to −20 °C, giving a yellow-orange microcrystalline solid, which was decanted, washed with hexane (3 × 3 mL approximately), and dried in vacuo, yielding 0.103 g (49%). IR (THF, cm^{-1}): 1941 vs, 1842 s. IR (KBr, cm^{-1}): 3314 m, 3271 m, 1933 s, 1837 s, 1572 m, 1420 w, 1372 w, 1284 w, 1159 w, 1020 w, 790 w. ^1H NMR (r.t.): 1.31 (s, H^{anti} methallyl, 2H), 2.06 (s, CH_3 methallyl, 3H), 2.13 (s, CH_3 dmpzH, 6H), 2.43 (br, CH_3 dmpzH, 6H), 3.35 (br, H^{syn} methallyl, 2H), 5.83 (br, H^4 dmpzH, 2H), 10.98 (br, N*H*, 1H), 11.41 (br, N*H*, 1H). ^1H NMR (233 K): 1.21 (s, H^{anti} methallyl, 1H), 1.37 (s, H^{anti} methallyl, 1H), 2.04 (s, CH_3 methallyl, 3H), 2.05 (s, CH_3 dmpzH, 3H), 2.21 (s, CH_3 dmpzH, 3H), 2.23 (s, CH_3 dmpzH, 3H), 2.80 (s, CH_3 dmpzH, 3H), 2.87 (d, J = 3.5 Hz, H^{syn} methallyl, 1H), 3.44 (d, J = 4.0 Hz, H^{syn} methallyl, 1H), 5.78 (s, H^4 dmpzH, 1H), 5.87 (s, H^4 dmpzH, 1H), 10.56 (s, N*H*, 1H), 11.32 (s, N*H*, 1H). $^{13}C\{^1H\}$ NMR: 10.7 (s, C^5H_3 dmpzH), 15.0 (br, C^3H_3 dmpzH), 20.4 (s, *C*H_3 methallyl), 52.3 (br, *C*H_2 methallyl), 61.5 (br, *C*H_2 methallyl), 84.9 (s, $CH_3C(CH_2)_2$), 106.6 (s, C^4 dmpzH), 139.7 (s, C^5 pzH), 152.0 (br, C^3 dmpzH), 153.8 (br, C^3 dmpzH), 225.0 (br, *C*O). Anal. Calcd. for $C_{16}H_{23}ClMoN_4O_2$: C, 44.20; H, 5.33; N, 12.88. Found: C, 44.51; H, 5.02; N, 13.06%. Crystals of **1b**·0.5(dmpzH$_2$)BF_4 were unexpectedly obtained after the reaction of [Mo(η^3-methallyl)Cl(CO)$_2$(NCMe)$_2$] with $TlBF_4$ and 3-fold excess of dmpzH in CH_2Cl_2.

4.4. [Mo(η^3-methallyl)(O_2CCH_3)(CO)$_2$(pzH)$_2$] (**2a**)

4.4.1. Method A

NaOAc $3H_2O$ (0.204 g, 1.5 mmol) and pzH (0.068 g, 1.0 mmol) were added to a solution of [Mo(η^3-methallyl)Cl(CO)$_2$(NCMe)$_2$] (0.162 g, 0.5 mmol) in THF (20 mL). The mixture was stirred at r.t. for 3 h. The volatiles were removed in vacuo and the orange residue was extracted with CH_2Cl_2 (ca. 30 ml) and filtered. Hexane was added (ca. 20 mL) and the solution was concentrated and cooled to −20 °C, giving a orange microcrystalline solid, which was decanted, washed with hexane (3 × 3 mL approximately), and dried in vacuo, yielding 0.101 g (51%) of **2a**.

4.4.2. Method B

NaOAc $3H_2O$ (0.030 g, 0.22 mmol) were added to a solution of **1a** (0.075 g, 0.2 mmol) in THF (10 mL). The mixture was stirred at r.t. for 3 h. Work-up as for Method A gave 0.045 g (56%) of **2a**. IR (THF, cm^{-1}): 1944 vs, 1847 s. IR (KBr, cm^{-1}): 3255 m, 3144 w, 2961 w, 2919 w, 1946 s, 1930 s, 1831 vs, 1612 s, 1527 m, 1474 m, 1394 s, 1332 m, 1254 w, 1139 m, 1048 m, 1025 w, 941 w, 900 w, 773 m, 660 w, 635 w, 609 w, 501 w. ^1H NMR (r.t.): 1.37 (s, H^{anti} methallyl, 2H), 1.71 (s, CH_3 methallyl, 3H), 2.11 (s, acetate, 3H), 3.11 (s, H^{syn} methallyl, 2H), 6.30 (s, H^4 pzH, 2H), 7.46 (s, $H^{5,3}$ pzH, 2H), 7.75 (s, $H^{3,5}$ pzH, 2H), 13.09 (br, N*H*, 2H). ^1H NMR (213 K): 1.11 (s, H^{anti} methallyl, 1H), 1.16 (s, H^{anti} methallyl, 1H), 1.64 (s, CH_3 methallyl, 3H), 1.90 (s, CH_3 acetate, 3H), 2.67 (s, H^{syn} methallyl, 1H), 3.24 (s, H^{syn} methallyl, 1H), 6.37 (s, H^4 pzH, 1H), 6.48 (s, H^4 pzH, 1H), 7.63 (s, H^5 pzH, 1H), 7.69 (s, H^5 pzH, 1H), 7.96 (s, H^3 pzH, 1H), 8.01 (s, H^3 pzH, 1H), 11.81 (br, N*H*, 1H), 14.95 (br, N*H*, 1H). $^{13}C\{^1H\}$ NMR: 19.2 (s, *C*H_3 methallyl), 25.6 (s, *C*H_3CO_2), 59.4 (s, *C*H_2 methallyl), 83.2 (s, $CH_3C(CH_2)_2$), 106.4 (s, C^4 pzH), 129.6 (s, $C^{5,3}$ pzH), 144.8 (s, $C^{3,5}$ pzH), 182,1 (s, CH_3CO_2), *C*O not observed. Anal. Calcd. for $C_{14}H_{18}MoN_4O_4$: C, 41.80; H, 4.51; N, 13.93. Found: C, 42.17; H, 4.34; N, 14.16%.

4.5. [Mo(η^3-methallyl)(O_2CCH_3)(CO)$_2$(dmpzH)$_2$] (**2b**)

NaOAc $3H_2O$ (0.122 g, 0.9 mmol) and dmpzH (0.058 g, 0.6 mmol) were added to a solution of [Mo(η^3-methallyl)Cl(CO)$_2$(NCMe)$_2$] (0.097 g, 0.3 mmol) in THF (15 mL). The mixture was stirred at r.t. for 2 h. Work-up as for **2a** gave 0.075 g (55%) of **2b** as a yellow microcrystalline solid. IR (THF, cm^{-1}): 1943 vs, 1846 s. IR (KBr, cm^{-1}): 3265 m, 3143 w, 3102 w, 3049 w, 2990 w, 2949 w, 2862w, 1935 vs, 1851 vs, 1588 s, 1569 s, 1492 w, 1474 w, 1394 s, 1335 m, 1306 w, 1272 m, 1160 w, 1042 w, 1028 m, 786 m, 741 w, 658 w, 633 w. ^1H NMR (r.t.): 1.26 (s, H^{anti} methallyl, 2H), 1.68 (s, CH_3 methallyl, 3H), 2.09 (s, CH_3 acetate, 3H), 2.19 (s, CH_3 dmpzH, 6H), 2.32 (s, CH_3 dmpzH, 6H), 3.01 (s, H^{syn} methallyl, 2H), 5.82 (s, H^4 dmpzH, 2H), 12.02 (br, N*H*, 2H). ^1H NMR (233 K): 1.23 (s, H^{anti} methallyl, 1H), 1.27 (s, H^{anti} methallyl, 1H), 1.57 (s, CH_3 methallyl, 3H), 1.99 (s, CH_3 acetate, 3H), 2.13 (s, CH_3 dmpzH, 6H), 2.26 (s, CH_3 dmpzH, 3H), 2.53 (s, CH_3 dmpzH, 3H), 2.80 (s, H^{syn} methallyl, 1H), 3.08 (s, H^{syn} methallyl, 1H), 5.77 (s, H^4 dmpzH, 1H), 5.86 (s, H^4 dmpzH, 1H), 11.13 (s, N*H*, 1H), 13.37 (s, N*H*, 1H). $^{13}C\{^1H\}$ NMR: 10.9 (s, *C*H_3 dmpzH), 14.5 (s, *C*H_3 dmpzH), 19.2 (s, *C*H_3 methallyl), 25.9 (s, *C*H_3CO_2), 59.6 (br, *C*H_2 methallyl), 84.3 (s, $CH_3C(CH_2)_2$), 106.1 (s, C^4 dmpzH), 140.2 (s, $C^{5,3}$ dmpzH), 151.2 (s, $C^{3,5}$ dmpzH), 180.9 (s, CH_3CO_2), *C*O not observed. Anal. Calcd. for $C_{18}H_{26}MoN_4O_4$: C, 47.17; H, 5.72; N, 12.23. Found: C, 46.92; H, 5.42; N, 12.00%.

Table 4
Crystal data and refinement details for **1a**, **1b**, **2a**, **2b**, **3a**, **3b**, **4a**, and **4b**.

	1a	**1b**·0.5(dmpzH$_2$)BF$_4$	**2a**	**2b**	**3a**	**3b**	**4a**·1/3CH$_2$Cl$_2$	**4b**·H$_2$O
Formula	$C_{12}H_{15}ClMoN_4O_2$	$C_{18.5}H_{27.5}B_{0.5}ClF_2MoN_5O_2$	$C_{14}H_{18}MoN_4O_4$	$C_{18}H_{26}MoN_4O_4$	$C_{11}H_{11}MnN_4O_5$	$C_{15}H_{19}MnN_4O_5$	$C_{11.33}H_{11.67}Cl_{0.67}N_4O_5Re$	$C_{15}H_{21}N_4O_6Re$
Formula weight	378.67	526.75	402.26	458.37	334.18	390.28	493.75	539.56
Crystal system	Monoclinic	Triclinic	Triclinic	Monoclinic	Orthorhombic	Monoclinic	Trigonal	Monoclinic
Space group	P2(1)/c	$P\bar{1}$	$P\bar{1}$	P2(1)/c	Pbca	P2(1)/n	$R\bar{3}$	P2(1)/n
a (Å)	8.8405(15)	9.860(3)	8.258(3)	15.256(11)	8.7526(15)	9.719(3)	20.588(6)	8.189(2)
b (Å)	12.536(2)	14.575(5)	8.718(3)	8.642(6)	14.772(3)	12.120(3)	20.588(6)	15.280(5)
c (Å)	14.352(2)	16.547(5)	24.840(8)	17.538(13)	22.892(4)	16.181(4)	22.435(12)	16.591(5)
α (°)	90	88.900(6)	97.538(6)	90	90	90	90	90
β (°)	105.059(3)	83.799(6)	90.339(6)	111.422(14)	90	96.116(5)	90	95.789(6)
γ (°)	90	79.213(5)	106.336(6)	90	90	90	120	90
V (Å^3)	1536.0(4)	2322.3(13)	1699.6(10)	2153(3)	2959.7(9)	1895.1(8)	8236(6)	2065.5(11)
Z	4	4	4	4	8	4	18	4
T (K)	296	298(2)	296	296	298	293	298	298
d_{calc} (g cm^{-3})	1.638	1.507	1.572	1.414	1.500	1.368	1.7929	1.735
F(000)	760	1076	816	944	1360	808	4212	1048
λ (Mo Kα) (Å)	0.71073	0.71073	0.71073	0.71073	0.71073	0.71073	0.71073	0.71073
Crystal size (mm)	0.09 × 0.20 × 0.22	0.32 × 0.16 × 0.08	0.36 × 0.32 × 0.31	0.34 × 0.30 × 0.11	0.36 × 0.25 × 0.11	0.40 × 0.25 × 0.11	0.37 × 0.12 × 0.08	0.40 × 0.12 × 0.06
Color	Yellow	Orange	Yellow	Yellow	Yellow	Yellow	Colorless	Colorless
μ (mm^{-1})	1.034	0.719	0.796	0.638	0.917	0.727	6.760	5.918
Scan range (°)	$2.19 \leqslant \theta \leqslant 23.28$	$1.24 \leqslant \theta \leqslant 25.56$	$0.83 \leqslant \theta \leqslant 23.30$	$1.43 \leqslant \theta \leqslant 23.36$	$1.78 \leqslant \theta \leqslant 25.35$	$2.10 \leqslant \theta \leqslant 23.27$	$1.46 \leqslant \theta \leqslant 26.00$	$1.82 \leqslant \theta \leqslant 23.29$
Absorption correction								
Corr. factors (max, min)	1.000000, 0.862373	1.000000, 0.678461	1.000000, 0.795048	1.000, 0.905541	1.000000, 0.810702	1.00000, 0.767878	1.00000, 0.462934	1.00000, 0.516102
No. of reflections measured	6659	16 557	7677	9327	22 334	8226	23 528	9521
No. of reflections independent [R(int)]	2197 [0.0224]	7900 [0.0420]	4846 [0.0166]	3121 [0.0219]	2716 [0.0435]	2721 [0.0243]	3609 [0.0407]	2959 [0.0249]
No of reflections observed, $I \geqslant 2\sigma(I)$	1925	5438	4588	2584	1798	2151	3047	2554
GOF on F^2	1.033	1.250	1.166	1.091	1.028	1.001	1.140	1.185
No. of parameters	190	548	436	259	194	239	233	241
Residuals R, wR_2	0.0228, 0.0585	0.0955, 0.2842	0.0320, 0.0757	0.0287, 0.0866	0.0486, 0.1440	0.0300, 0.0832	0.0232, 0.0697	0.0292, 0.0949

4.6. *fac*-[Mn(O_2CCH_3)(CO)$_3$(pzH)$_2$] (**3a**)

To a recently prepared solution of *fac*-[MnBr(CO)$_3$(NCMe)$_2$] (obtained from 0.082 g of [MnBr(CO)$_5$], 0.3 mmol) in THF (15 mL), AgOAc (0.055 g, 0.33 mmol) and then pzH (0.042 g, 0.6 mmol) were added. The solution was stirred for 5 min. Work-up as for **2a** gave 0.075 g (75%) of **3a** as a yellow microcrystalline solid. IR (THF, cm^{-1}): 2033 vs 1938 vs, 1912 vs. IR (KBr, cm^{-1}): 3344 w, 3158 w, 2026 vs, 1918 vs br, 1608 m, 1534 m, 1471 m, 1387 m, 1355 w, 1335 m, 1261 m, 1163 w, 1134 m, 1059 m, 1048 m, 942 w, 910 w, 864 w, 759 m, 698 w, 664 w, 634 w, 599 w, 521 w. ^{1}H NMR: 2.24 (br, acetate, 3H), 6.37 (s, *H*^{4} pzH, 2H), 7.59 (br, *H*^{3} pzH, 2H), 7.63 (s, *H*^{5} pzH, 2H), 13.04 (br, N*H*, 2H). ^{13}C{^{1}H} NMR [$(CD_3)_2CO$] [33]: 28.1 (s, *C*H$_3$CO$_2$), 108.4 (s, *C*^{4} pzH), 132.7 (s, *C*^{5,3} pzH), 143.7 (s, *C*^{3,5} pzH), 170.0 (s, CH$_3$*C*O$_2$), 222.2 (s, 1*C*O), 223.3 (s, 2*C*O). Conduct. Λ_M (Me_2CO): 2 S cm^2 mol^{-1}. Anal. Calcd. for $C_{11}H_{11}MnN_4O_5$: C, 39.54; H, 3.32; N, 16.77. Found: C, 39.21; H, 2.97; N, 17.07%.

4.7. *fac*-[Mn(O_2CCH_3)(CO)$_3$(dmpzH)$_2$] (**3b**)

To a recently prepared solution of *fac*-[MnBr(CO)$_3$(NCMe)$_2$] (obtained from 0.137 g of [MnBr(CO)$_5$], 0.5 mmol) in THF (20 mL), AgOAc (0.091 g, 0.55 mmol) and then dmpzH (0.097 g, 1.0 mmol) were added. The solution was stirred for 45 min. Work-up as for **2a** gave 0.152 g (78%) of **3b** as a yellow microcrystalline solid. IR (THF, cm^{-1}): 2030 vs, 1934 vs, 1906 vs. IR (KBr, cm^{-1}): 3313 w, 3271 w, 2930 w, 2029 vs, 1934 vs, 1898 vs, 1571 s, 1543 w, 1400 s, 1289 m, 1142 w, 1043 w, 806 m, 688 w, 662 w, 632 w, 518 w. ^{1}H NMR: 2.13 (s, C*H*$_3$ dmpzH, 6H), 2.17 (s, C*H*$_3$ acetate, 3H), 2.23 (s, C*H*$_3$ dmpzH, 6H), 5.84 (s, H^4 dmpzH, 2H), 12.02 (br, N*H*, 2H). ^{13}C{^{1}H} NMR: 11.5 (s, ^{5}CH$_3$ dmpzH), 13.9 (s, ^{3}CH$_3$ dmpzH), 26.0 (br, *C*H$_3$CO$_2$), 106.9 (s, *C*^{4} dmpzH), 141.0 (s, *C*^{5,3} dmpzH), 153.1 (s, *C*^{3,5} dmpzH), 184.5 (br, CH$_3$*C*O$_2$), 219.7 (s, 2*C*O), 223.1 (s, 1*C*O). Conduct. Λ_M (Me_2CO): 0 S cm^2 mol^{-1}. Anal. Calcd. for $C_{15}H_{19}MnN_4O_5$: C, 46.16; H, 4.90; N, 14.36. Found: C, 45.81; H, 4.63; N, 14.04%.

4.8. *fac*-[Re(O_2CCH_3)(CO)$_3$(pzH)$_2$] (**4a**)

To a solution of *fac*-[ReBr(CO)$_3$(NCMe)$_2$] (0.127 g, 0.3 mmol) in Me_2CO (10 mL), AgOAc (0.055 g, 0.33 mmol) and then pzH (0.042 g, 0.6 mmol) were added. The solution was stirred for 30 min. Work-up as for **2a** gave 0.115 g (84%) of **4a** as a colorless microcrystalline solid. IR (THF, cm^{-1}): 2024 vs, 1914 vs, 1894 vs. IR (KBr, cm^{-1}): 3145 w, 2989 w, 2875 w, 2027 vs, 1903 vs br, 1570 s, 1528 s, 1482 s, 1404 s, 1353 s, 1272 m, 1164 m, 1142 s, 1064 s, 1051 s, 1020 w, 951 w, 912 w, 882 w, 880 w, 807 m, 766 s, 672 m, 659 w, 635 w, 608 m, 531 m, 488 m. ^{1}H NMR: 2.18 (s, acetate, 3H), 6.35 (s, *H*^{4} pzH, 2H), 7.58 (s, *H*^{3,5} pzH, 2H), 7.62 (s, *H*^{5,3} pzH, 2H), 12.94 (br, N*H*, 2H).^{13}C{^{1}H} NMR [$(CD_3)_2CO$]:[43] 23.9 (s, *C*H$_3$CO$_2$), 107.6 (s, *C*^{4} pzH), 131.9 (s, *C*^{5,3} pzH), 143.0 (s, *C*^{3,5} pzH), 180.8 (s, CH$_3$*C*O$_2$), 196.9 (2*C*O), 206.1 (partially overlapped with the acetone signal, *C*O). Conduct. Λ_M (Me_2CO): 2 S cm^2 mol^{-1}. Anal. Calcd. for $C_{11}H_{11}N_4O_5Re$: C, 28.39; H, 2.38; N, 12.04. Found: C, 28.73; H, 2.67; N, 11.72%.

4.9. *fac*-[Re(O_2CCH_3)(CO)$_3$(dmpzH)$_2$] (**4b**)

To a solution of *fac*-[ReBr(CO)$_3$(NCMe)$_2$] (0.216 g, 0.5 mmol) in Me_2CO (20 mL), AgOAc (0.092 g, 0.55 mmol) and then dmpzH (0.097 g, 1.0 mmol) were added. The solution was stirred for 40 min. Work-up as for **2a** gave 0.239 g (92%) of **4b** as a colorless microcrystalline solid. IR (THF, cm^{-1}): 2021 vs, 1911 vs, 1886 vs. IR (KBr, cm^{-1}): 3398 s, 2929 w, 2017 vs, 1897 vs br, 1576 m, 1395 m, 1337 m, 1309 w, 1824 w, 1176 w, 1152 w, 1101 w, 1048 m, 1027 m, 882 w, 800 w, 664 m, 503 w. ^{1}H NMR: 2.12 (s, C*H*$_3$ acetate, 3H), 2.14 (s, C*H*$_3$ dmpzH, 6H), 2.25 (s, C*H*$_3$ dmpzH, 6H), 5.87 (s, *H*^{4} dmpzH, 2H), 12.02 (br, N*H*, 2H). ^{13}C{^{1}H} NMR: 11.1 (s, ^{5}*C*H$_3$ dmpzH), 14.2 (s, ^{3}*C*H$_3$ dmpzH), 24.2 (s, *C*H$_3$CO$_2$), 106.1 (s, *C*^{4} dmpzH), 141.2 (s, *C*^{5,3} dmpzH), 152.6 (s, *C*^{3,5} dmpzH), 181.6 (s, CH$_3$*C*O$_2$), 195.3 (s, 2*C*O), 195.8 (s, 1*C*O). Conduct. Λ_M (Me_2CO): 0 S cm^2 mol^{-1}. Anal. Calcd. for $C_{15}H_{19}N_4O_5Re$: C, 34.54; H, 3.67; N, 10.74. Found: C, 34.34; H, 3.31; N, 10.47%.

4.10. Crystal structure determination for compounds **1a, 1b, 2a, 2b, 3a, 3b, 4a**, and **4b**

Crystals were grown by slow diffusion of hexane into concentrated solutions of the complexes in CH_2Cl_2 at −20 °C. Relevant crystallographic details are given in Table 4. A crystal was attached to a glass fiber and transferred to a Bruker AXS SMART 1000 diffractometer with graphite monochromatized Mo Kα X-radiation and a CCD area detector. Raw frame data were integrated with the SAINT program [34]. The structure was solved by direct methods ith SHELXTL [35]. A semi-empirical absorption correction was applied with the program SADABS [36]. All non-hydrogen atoms were refined anisotropically. Hydrogen atoms were set in calculated positions and refined as riding atoms, with a common thermal parameter. All calculations and graphics were made with SHELXTL. For **4a** several peaks were found in the proximity of the trigonal axis. After several attempts, they were modelled as two disordered molecules of dichloromethane with the carbon atoms lying in the trigonal axis, they were refined as rigid groups with occupancy factors of one-sixth each. Distances and angles of hydrogen bonds were calculated with PARST [37] (normalized values) [38].

5. Supplementary material

CCDC 716936, 716937, 716938, 716939, 716940, 716941, 716942 and 716943 contain the supplementary crystallographic data for this paper. These data can be obtained free of charge from The Cambridge Crystallographic Data Centre via www.ccdc.cam.ac.uk/data_request/cif.

Acknowledgments

The authors thank the Spanish Ministerio de Educación y Ciencia (CTQ2006-08924) and the Junta de Castilla y León (VA070A08) for financial support. M.A. and R.G.-R. thank the MEC (Program FPI) for a grant. We also thank Dr. Celedonio Alvarez for helpful discussions.

References

[1] Some examples of chains: (a) R. Graziani, U. Casellato, R. Ettorre, G. Plazzogna, J. Chem. Soc., Dalton Trans. (1982) 805–808;
(b) J.D. Crane, O.D. Fox, E. Sinn, J. Chem. Soc., Dalton Trans. (1999) 1461–1465;
(c) K. Sakai, Y. Tomita, T. Ue, K. Goshima, M. Ohminato, T. Tsubomura, K. Matsumoto, K. Ohmura, K. Kawakami, Inorg. Chim. Acta 297 (2000) 64–71;
(d) A. Chadghan, J. Pons, A. Caubet, J. Casabó, J. Ros, A. Alvarez-Larena, J.F. Piniella, Polyhedron 19 (2000) 855–862.
[2] Some examples of dimers: (a) M.A. Cinellu, S. Stoccoro, G. Minghetti, A.L. Bandini, G. Banditelli, B. Bovio, J. Organomet. Chem. 372 (1989) 311–325;
(b) M. Munakata, L.P. Wu, M. Yamamoto, T. Kuroda-Sowa, M. Maekawa, S. Kawata, S. Kitagawa, J. Chem. Soc., Dalton Trans. (1995) 4099–4106;
(c) G.A. Ardizzoia, G. La Monica, S. Cenini, M. Moret, N. Masciocchi, J. Chem. Soc., Dalton Trans. (1996) 1351–1357;
(d) I.A. Guzei, C.H. Winter, Inorg. Chem. 36 (1997) 4415–4420;
(e) S.M. Couchman, J.C. Jeffery, M.D. Ward, Polyhedron 18 (1999) 2633–2640.
[3] (a) S. Nieto, J. Pérez, L. Riera, V. Riera, D. Miguel, J.A. Golen, A.L. Rheingold, Inorg. Chem. 46 (2007) 3407–3418;
(b) S. Nieto, J. Pérez, L. Riera, V. Riera, D. Miguel, Chem. Eur. J. 12 (2006) 2244–2251;
(c) S. Nieto, J. Pérez, V. Riera, D. Miguel, C. Alvarez, Chem. Commun. (2005) 546–548;

(d) S.L. Renard, C.A. Kilner, J. Fisher, M.A. Halcrow, J. Chem. Soc., Dalton Trans. (2002) 4206–4212;
(e) X. Liu, C.A. Kilner, M.A. Halcrow, Chem. Commun. (2002) 704–705;
(f) D.L. Reger, Y. Ding, A.L. Rheingold, R.L. Ostrander, Inorg. Chem. 33 (1994) 4226–4230;
(g) A. Looney, G. Parkin, A.L. Rheingold, Inorg. Chem. 30 (1991) 3099–3101.
[4] (a) D. Braga, J. Chem. Soc., Dalton Trans. (2000) 3705–3713;
(b) G.R. Desiraju, J. Chem. Soc., Dalton Trans. (2000) 3745–3751.
[5] See for example: (a) M. Tadokoro, T. Inoue, S. Tamaki, K. Fujii, K. Isogai, H. Nakazawa, S. Takeda, K. Isobe, N. Koga, A. Ichimura, K. Nakasuji, Angew. Chem., Int. Ed. 46 (2007) 5938–5942;
(b) S. Shibahara, H. Kitagawa, Y. Ozawa, K. Toriumi, T. Kubo, K. Nakasuji, Inorg. Chem. 46 (2007) 1162–1170.
[6] (a) S. Derossi, H. Adams, M.D. Ward, Dalton Trans. (2007) 33–36;
(b) V. Coué, R. Dessapt, M. Bujoli-Doeuff, M. Evain, S. Jobic, Inorg. Chem. 46 (2007) 2824–2835;
(c) O. Sato, Acc. Chem. Res. 36 (2003) 692–700;
(d) E.H.A. Beckers, P.A. van Hal, A.P.H.J. Schenning, A. El-ghayoury, E. Peeters, M.T. Rispens, J.C. Hummelen, E.W. Meijer, R.A.J. Janssen, J. Mater. Chem. 12 (2002) 2054–2060.
[7] C. Desplanches, E. Ruiz, S. Alvarez, Chem. Commun. (2002) 2614–2615.
[8] (a) S. Kitagawa, K. Uemura, Chem. Soc. Rev. 34 (2005) 109–119;
(b) S. Kitagawa, R. Kytaura, S. Noro, Angew. Chem., Int. Ed. 43 (2004) 2334–2375;
(c) F. Zhang, M.C. Jennings, R.J. Puddephatt, Chem. Commun. (2007) 1496–1498;
(d) M. Du, X.-J. Yiang, X.-J. Zhao, Inorg. Chem. 46 (2007) 3984–3995;
(e) N.L. Rosi, J. Kim, M. Eddaoudi, B. Chen, M. O'Keefe, O.M. Yaghi, J. Am. Chem. Soc. 127 (2005) 1504–1518.
[9] See for example: (a) D.B. Grotjahn, Chem. Eur. J. 11 (2005) 7146–7153;
(b) K. Abdur-Raschid, R. Abbel, A. Hadzovic, A.J. Lough, R.H. Morris, Inorg. Chem. 44 (2005) 2483–2492;
(c) W.K. Fung, X. Huang, M.L. Man, S.M. Ng, M.Y. Hung, Z. Lin, C.P. Lau, J. Am. Chem. Soc. 125 (2003) 11539–11544.
[10] (a) M. Arroyo, A. López-Sanvicente, D. Miguel, F. Villafañe, Eur. J. Inorg. Chem. (2005) 4430–4437;
(b) P. Paredes, D. Miguel, F. Villafañe, Eur. J. Inorg. Chem. (2003) 995–1004;
(c) G.A. Ardizzoia, G. LaMonica, A. Maspero, M. Moret, N. Masciocchi, Eur. J. Inorg. Chem. (1998) 1503–1512.
[11] (a) E. Szajna-Fuller, B.M. Chambers, A.M. Arif, L.M. Berreau, Inorg. Chem. 46 (2007) 5486–5498;
(b) E. Szajna, A.M. Arif, L.M. Berreau, J. Am. Chem. Soc. 127 (2005) 17186–17187.
[12] The synthesis of the allyl complex similar to **1b** has been recently described by a different method, but no complete spectroscopic or structural characterization was given (Ref. [3a]).
[13] **1b** crystallized as **1b**·0.5($dmpzH_2$)BF_4 (see Section 4), and contains two crystallographically independent but chemically equivalent molecules, their distances and angles being very similar. Fig. 1 and Table 1 collect one of them. Complete Tables for the two molecules can be found in the CIF. Due to the low quality of the crystal, the resulting determination is poor (high residuals). Nevertheless, the structure is included here since it confirms unambiguously the connectivity of the molecule.
[14] M.D. Curtis, O. Eisenstein, Organometallics 3 (1984) 887–895.
[15] F.A. Cotton, R.L. Luck, Acta Crystallogr., Sect. C 46 (1990) 138–140.
[16] (a) R. Davis, L.A.P Kane-Maguire, in: G. Wilkinson, F.G.A. Stone, E.W. Abel (Eds.), Comprehensive Organometallic Chemistry, vol. 8, Pergamon, Oxford, UK, 1982, pp. 1156–1159;
(b) M.W. Whiteley, in: E.W. Abel, F.G.A. Stone, G. Wilkinson (Eds.), Comprehensive Organometallic Chemistry II, vol. 12, Pergamon, Oxford, UK, 1995, pp. 337–338.
[17] (a) G.A. Jeffrey, An Introduction to Hydrogen Bonding, Oxford University Press, New York, 1997 (Chapter 2);
(b) T. Steiner, Angew. Chem., Int. Ed. 41 (2002) 48–76.
[18] **1b** crystallized out incorporating one-half of the ionic pair ($dmpzH_2$)BF_4 per molecule of **1b**. The pyrazolium ion is involved in strong hydrogen bonds with the chlorido ligands: H(90)···Cl(1) 1.587 Å and H(91)···Cl(51) 1.548 Å, N···Cl distances 2.598 Å and 2.573 Å, and N–H···Cl angles 166° and 173°, respectively.
[19] For **2a**, two crystallographically independent but chemically equivalent molecules were found in the asymmetric unit, with their distances and angles being very similar. Fig. 2 and Table 2 collect one of them. Complete tables for the two molecules can be found in the CIF.
[20] (a) N.I. Pyshnograeva, V.N. Setkina, V.G. Andrianov, Y.T. Struchkov, D.N. Kursanov, J. Organomet. Chem. 186 (1980) 331–338;
(b) S.U. Son, K.H. Park, Y.K. Chung, Organometallics 19 (2000) 5241–5243;
(c) W.-Y. Wong, W.-K. Wong, C. Sun, W.-T. Wong, J. Organomet. Chem. 612 (2000) 160–171.
[21] However, the solid state C–O frequencies of **1a** state are slightly lower than those of **1b** (see Section 2). This feature was also observed for the complexes [Mo(η^3-allyl)Br$(CO)_2L_2$] (L = pzH, dmpzH), and could be explained considering either lattice effects, and/or weak intermolecular hydrogen bonds involving the NH atoms and the oxygens of the carbonyls (Ref. [10b]).
[22] J.W. Faller, D.A. Haitko, R.D. Adams, D.F. Chodosh, J. Am. Chem. Soc. 101 (1979) 865–876.
[23] (a) S.K. Chowdhury, M. Nandi, V.S. Joshi, A. Sarkar, Organometallics 16 (1997) 1806–1809;
(b) D.S. Frohnapfel, P.S. White, J.L. Templeton, H. Rüegger, P.S. Pregosin, Organometallics 16 (1997) 3737–3750;
(c) K.-B. Shiu, C.-J. Chang, Y. Wang, M.-C. Cheng, J. Organomet. Chem. 406 (1991) 363–369.
[24] P. Espinet, R. Hernando, G. Iturbe, F. Villafañe, G.A. Orpen, I. Pascual, Eur. J. Inorg. Chem. (2000) 1031–1038.
[25] D.R. van Staveren, E. Bill, E. Bothe, M. Bühl, T. Weyhermüller, N. Metzler-Nolte, Chem. Eur. J. 8 (2002) 1649–1662.
[26] (a) D. Carmona, J. Ferrer, J.M. Arilla, J. Reyes, F.J. Lahoz, S. Elipe, F.J. Modrego, L.A. Oro, Organometallics 19 (2000) 798–808;
(b) D. Röttger, G. Erker, M. Grehl, R. Fröhlich, Organometallics 13 (1994) 3897–3902;
(c) D. Carmona, J. Ferrer, L.A. Oro, M.C. Apreda, C. Foces-Foces, F.H. Cano, J. Elguero, M.L. Jimeno, J. Chem. Soc., Dalton Trans. (1990) 1463–1476;
(d) D. Carmona, L.A. Oro, M.P. Lamata, J. Elguero, M.C. Apreda, C. Foces-Foces, F.H. Cano, Angew. Chem., Int. Ed. Eng. 25 (1986) 1114–1115.
[27] R. Contreras, M. Valderrama, E.M. Orellana, D. Boys, D. Carmona, L.A. Oro, M.P. Lamata, J. Ferrer, J. Organomet. Chem. 606 (2000) 197–202.
[28] T. Beringhelli, G. D'Alfonso, M. Panigati, F. Porta, P. Mercandelli, M. Moret, A. Sironi, Organometallics 17 (1998) 3282–3292.
[29] D.D. Perrin, W.L.F Armarego, Purification of Laboratory Chemicals, 3rd ed., Pergamon Press, Oxford, 1988.
[30] H. Tom Dieck, H. Friedel, J. Organomet. Chem. 14 (1968) 375–385.
[31] M.F. Farona, K.F. Kraus, Inorg. Chem. 9 (1970) 1700–1704.
[32] W. Geary, Coord. Chem. Rev. 7 (1971) 81–122.
[33] No signals from the acetate group are detected in the ^{13}C NMR spectrum in $CDCl_3$ due to their extreme broadness.
[34] SAINT+. SAX Area Detector Integration Program. Version 6.02, Bruker AXS Inc., Madison, WI, 1999.
[35] G.M. Sheldrick, SHELXTL, An Integrated System for Solving, Refining, and Displaying Crystal Structures from Diffraction Data, Version 5.1, Bruker AXS Inc., Madison, WI, 1998.
[36] G.M. Sheldrick, SADABS, Empirical Absorption Correction Program, University of Göttingen, Göttingen, Germany, 1997.
[37] M. Nardelli, Comp. Chem. 7 (1983) 95–98;
M. Nardelli, J. Appl. Cryst. 28 (1995) 659.
[38] (a) G.A. Jeffrey, L. Lewis, Carbohydr. Res. 60 (1978) 179–182;
(b) R. Taylor, O. Kennard, Acta Crystallogr. B39 (1983) 133–138.